Structural analysis of Buti's bell tower

Katia Bernardeschi

Istituto di Scienza e Tecnologie dell'Informazione "Alessandro Faedo", ISTI-CNR

Via G. Moruzzi, 1 56124 Pisa Italy, tel. +39 050 3152932, fax +39 050 3138091,

e-mail: katia.bernardeschi@guest.cnuce.cnr.it

Cristina Padovani

Istituto di Scienza e Tecnologie dell'Informazione "Alessandro Faedo", ISTI-CNR

Via G. Moruzzi, 1 56124 Pisa Italy, tel. +39 050 3152951, fax +39 050 3138091,

e-mail: cristina.padovani@cnuce.cnr.it

Giuseppe Pasquinelli

Istituto di Scienza e Tecnologie dell'Informazione "Alessandro Faedo", ISTI-CNR

Via G. Moruzzi, 1 56124 Pisa Italy, tel. +39 050 3152950, fax +39 050 3138091,

e-mail: giuseppe.pasquinelli@cnuce.cnr.it

Abstract.

The paper describes the numerical techniques implemented in the finite-element code NOSA for structural analysis of masonry constructions.

The code is then applied to the analysis of "Buti's bell tower", a medieval structure located on the Pisa mountains, under two different conditions: firstly, with the structure subjected to its own weight alone, and then while subjected to both its own weight and a horizontal load, which models an earthquake. The displacement and stress fields, as well as the distribution of cracking have been calculated with NOSA and the numerical results analysed and compared to the actual distribution of fractures in the tower.

Keywords: **Masonry constructions/ finite-element analysis/ seismic analysis**

1. Research aims

Over the last two decades, constitutive models and calculation techniques have become available that enable realistic description of the static behaviour of masonry structures.

Recent studies [1], [2], [3], [4] have led to a better understanding of the constitutive equation of the materials not withstanding tension, known in literature as *masonry-like* materials. Such equation can realistically reproduce the mechanical behaviour of masonry, at least regarding certain aspects. Within this framework, masonry is considered to be a non-linear elastic material, with zero tensile strength and infinite compressive strength.

In order to study real problems, the equilibrium problem of masonry structures can be solved via the finite-element method. To this end, suitable numerical techniques have been developed [4], [5], [6] and [7]. They are based on the Newton-Raphson method for solving the non-linear system obtained through discretising the structure into finite elements. Their application requires that the derivative of the stress with respect to the strain be explicitly known, as this is needed in order to calculate the tangent stiffness matrix.

The numerical method studied has therefore been implemented into the finite-element code NOSA developed at ISTI-CNR [8], [9], which allows determination of the stress state and the presence of any cracking, and moreover enables modelling to be performed of any

potential consolidation and restoration work, such as, for example, the fitting of chains [10].

The code has been successfully applied to the analysis of some buildings of historical and architectural interest, amongst which the chimney of the Vecchi Macelli in Pisa [11], the S. Nicolò's Motherhouse in Noto [12], the Goldoni Theatre in Livorno [13], the Medici Arsenal in Pisa [14], [15] and the Baptistery of the Volterra Cathedral [16] deserve special mention.

In this paper we apply the numerical techniques and the finite-element code NOSA to studying the structural behaviour of the medieval tower known as "Buti's bell tower". The aim is to highlight the potentialities of this computational tool, which can be used both to evaluate the safety of masonry monuments, as well as to guide the choice of restoration operations.

Section 2 deals with the numerical method used for solution of the equilibrium problem of masonry structures and implemented in the NOSA code. In particular, the constitutive equation of masonry-like materials and the finite-element procedure implemented in the NOSA code are briefly recalled. Finally, the brick and shell elements employed to discretise the bell tower and its vault are described.

In Section 3, after a brief historical note on the bell tower, a geometrical description of the structure is provided, and an analysis of acting loads carried out. We then take up the numerical analyses conducted with the NOSA code. Two analyses have been performed: the first by discretising the bell tower with brick elements, the second with shell elements. In both cases, the bell tower is subjected to its own weight and a horizontal load that models the action of an earthquake. According to the guidelines in technical regulations, the magnitude of the lateral load is 7 % of the total weight [17].

The stress field calculated with NOSA fits in well with the observed distribution of cracks in the bell tower. The numerical results accurately indicates the presence of fractures in the tower shaft and their absence in the vault.

The finite-element analysis highlights that the compressive stresses in the structure are well below the material's compressive strength, according to the fact that no crushing fractures are presents in any region of the structure.

2. The numerical method

2.1 The constitutive equation

In order to model the constitutive behaviour of the masonry material, it is assumed to be a non-linear hyperelastic material with zero tensile strength and infinite compressive strength. More precisely, it is supposed that the infinitesimal strain $\mathbf{E}$ is the sum of two parts: an elastic part $\mathbf{E}^e$ and a positive semi-definite inelastic strain $\mathbf{E}^a$; $\mathbf{E} = \mathbf{E}^e + \mathbf{E}^a$. Moreover, the stress $\mathbf{T}$, negative semi-definite and orthogonal to $\mathbf{E}^a$, depends linearly and isotropically on $\mathbf{E}^e$, $\mathbf{T} = \frac{E}{1+\nu}\mathbf{E}^e + \frac{\nu E}{(1+\nu)(1-2\nu)} tr(\mathbf{E}^e)\mathbf{I}$, with E and ν the Young's modulus and the Poisson's ratio of the material. Such a material is usually called *masonry-like* or *no-tension* material. It is possible to express the stress tensor $\mathbf{T}$ as function of the total strain $\mathbf{E}$, $\mathbf{T} = \hat{\mathbf{T}}(\mathbf{E})$, with $\hat{\mathbf{T}}$ a non-linear function. By using the coaxiality of $\mathbf{E}$, $\mathbf{T}$ and $\mathbf{E}^a$, function $\hat{\mathbf{T}}$ can be easily calculated for both the two- and three-dimensional case.

Tensor $\mathbf{E}^a$ can be interpreted as fracture strain. In fact, if $\mathbf{E}^a$ is non-null in any region of the structure, then we can expect fractures to be present in that region. Nevertheless, a simple analysis of the components of $\mathbf{E}^a$ does not generally yield any information about the direction of eventual fractures. To this end, it should be noted that if for any vector $\mathbf{v}$ it holds that $\mathbf{v} \cdot \mathbf{E}^a \mathbf{v} > 0$, then $\mathbf{v}$ is not necessarily a fracture direction. Nonetheless, there must surely exist at least one eigenvector $\mathbf{q}$ of $\mathbf{E}^a$ such that $\mathbf{q} \cdot \mathbf{E}^a \mathbf{q} > 0$ and then, by virtue of the orthogonality of $\mathbf{E}^a$ and $\mathbf{T}$, $\mathbf{q} \cdot \mathbf{T}\mathbf{q} = 0$. Thus, we can infer that if Φ is a fracture surface, then every vector orthogonal to Φ is an eigenvector of $\mathbf{T}$ corresponding to the eigenvalue 0. This criterion has been used to reveal the presence and corresponding direction of fractures in specific regions of the bell tower.

2.2 The finite element procedure

The numerical solution to equilibrium problems of masonry structures is obtained via the finite-element method. In particular, numerical techniques based on the Newton-Raphson

method are applied to solve the non-linear system obtained by discretising the structure into finite elements. In order to calculate the tangent stiffness matrix the derivative $D_E\hat{\mathbf{T}}$ of the stress with respect to the strain must be explicitly calculated.

Because of the non-linearity of the constitutive equation, the loads are applied incrementally to the structure, a technique that has proved to be essential not only to studying the bell tower in question, but also to the analysis of structures near collapse [5].

The constitutive equation of masonry-like materials and the numerical techniques for the structural analysis of masonry structures have been implemented in the finite-element code NOSA. Here, we recall the algorithm implemented in NOSA.

Let us consider the following quantities related to the *i*t iteration of the *j*th load increment:

$\mathbf{u}^{(i,j)}$	vector of nodal displacements,
$\mathbf{D}(\mathbf{u}^{(i,j)})$	matrix of the engineering components of $D_E\hat{\mathbf{T}}$,
$\mathbf{K}_T(\mathbf{u}^{(i,j)})$	tangent stiffness matrix,
$\mathbf{f}^{(i,j)}$	nodal equivalent of the assigned incremental load if $i = 0$; nodal equivalent of residual load if $i \geq 1$,
$\mathbf{e}_G{}^{(i,j)}$	vector of the engineering components of the total strain,
$\mathbf{a}_G{}^{(i,j)}$	vector of the engineering components of the fracture strain,
$\mathbf{t}_G{}^{(i,j)}$	vector of the engineering components of the stress,

where the subscript G indicates the Gauss point at which these quantities are calculated.

At the first iteration of the first load increment, $\mathbf{u}^{(0,1)} = \mathbf{0}$, and $\mathbf{D}(\mathbf{u}^{(0,1)})$ coincides with the linear elastic matrix. Let us assume that during the *j*th load increment, we have calculated the displacement $\mathbf{u}^{(i,j)}$, the tangent stiffness matrix $\mathbf{K}_T(\mathbf{u}^{(i,j)})$ and the nodal equivalent loads $\mathbf{f}^{(i,j)}$ corresponding to the *i*th iteration. We then solve the linear algebraic system

$$\mathbf{K}_T(\mathbf{u}^{(i,j)})\Delta\mathbf{u}^{(i,j)} = \mathbf{f}^{(i,j)}, \tag{1}$$

in order to determine the displacement $\mathbf{u}^{(i+1,j)} = \mathbf{u}^{(i,j)} + \Delta\mathbf{u}^{(i,j)}$, corresponding to the (*i*+1)th iteration.

Then, for every Gauss point of every element we calculate the total strain $\mathbf{e}_G^{(i+1,j)}$ associate with the displacement $\mathbf{u}^{(i+1,j)}$, and its eigenvalues which are needed to calculate the inelastic strain $\mathbf{a}_G^{(i+1,j)}$; after which we calculate the stress $\mathbf{t}_G^{(i+1,j)}$ using the constitutive equation of masonry-like materials described in Section 2.1. Moreover, using the explicit expression for $D_E\hat{\mathbf{T}}$ [5], [6], we arrive at matrix $\mathbf{D}(\mathbf{u}^{(i+1,j)})$, which may be used as needed in the next iteration or load increment.

Finally, we calculate the vector of residual loads $\mathbf{f}^{(i+1,j)}$ and perform the convergence check

$$\frac{|\mathbf{f}^{(i+1,j)}|}{\sum_{k=1}^{j}|\mathbf{f}^{(0,k)}|} \leq \xi; \tag{2}$$

if convergence has not been reached, we repeat all operations beginning with the solution to system (1).

2.3 Numerical modelling

The bell tower has been discretised with eight-nodes brick elements. A further finite element analysis has been performed using thin shell elements [18], [19], which are especially well-suited to modelling thin structures, such as vaults, walls, *etc*. These quadrilateral eight-node elements are non-conforming: in fact, rotations of the mid-side nodes are independent of displacements of the corner nodes. Thin shell elements are based on three hypotheses: that displacements and strains are infinitesimal; the unit vector **n**, orthogonal to the mean surface of the shell, maintains its length after deformation; and that after deformation, the normal vector **n** becomes the unit vector orthogonal to the mean surface of the deformed shell (Love-Kirchhoff hypothesis). Moreover, a plane stress state is assumed.

Let us consider a vault element with thickness *h*, Let η_1, η_2 be an orthogonal co-ordinate system (not necessarily the principal one) defined on the means surface with ζ as the co-ordinate in the normal direction **n**. For each point having co-ordinates (η_1, η_2, ζ) and for

each unit vector $\mathbf{g}(\alpha) = (\cos\alpha, \sin\alpha)$ in the plane tangent to the mean surface, where $\alpha \in [-\pi/2, \pi/2)$ is the angle formed by $\mathbf{g}(\alpha)$ with the direction η_1, let us put

$$\sigma(\alpha, \zeta) = \mathbf{g}(\alpha) \cdot \mathbf{T}(\zeta)\mathbf{g}(\alpha), \tag{3}$$

where $\mathbf{T}(\zeta)$ is the stress tensor at the point with co-ordinates (η_1, η_2, ζ). Thus, the relations

$$N(\alpha) = \int_{-h/2}^{h/2} \sigma(\alpha, \zeta)\, \mathrm{d}\zeta, \quad M(\alpha) = \int_{-h/2}^{h/2} \sigma(\alpha, \zeta)\zeta\, \mathrm{d}\zeta \tag{4}$$

respectively define the normal force and the bending moment per unit length corresponding to $\mathbf{g}(\alpha)$. In view of the fact that $\mathbf{T}$ is negative semi-definite, $N(\alpha)$ is non-positive for every α. Let $\mathbf{g}_1 = \mathbf{g}(0)$ and $\mathbf{g}_2 = \mathbf{g}(\pi/2)$ be the unit vectors tangent to axes η_1 and η_2 axis, respectively. Thus, we have $\mathbf{T}(\zeta) = \begin{bmatrix} \sigma_1(\zeta) & \tau(\zeta) \\ \tau(\zeta) & \sigma_2(\zeta) \end{bmatrix}$ with respect to the basis $\mathbf{g}_1, \mathbf{g}_2$, and from (3), the relation $\sigma(\alpha, \zeta) = \sigma_1(\zeta)\cos^2\alpha + \sigma_2(\zeta)\sin^2\alpha + 2\tau(\zeta)\sin\alpha\cos\alpha$ holds for each $\alpha \in [-\pi/2, \pi/2)$.

By taking (4) into account, we obtain $N(\alpha) = N_1 \cos^2\alpha + N_2 \sin^2\alpha + N_{12} \sin 2\alpha$, where $N_1 = \int_{-h/2}^{h/2} \sigma_1(\zeta)\, \mathrm{d}\zeta$, $N_2 = \int_{-h/2}^{h/2} \sigma_2(\zeta)\, \mathrm{d}\zeta$, $N_{12} = \int_{-h/2}^{h/2} \tau(\zeta)\, \mathrm{d}\zeta$. Analogously, setting $M_1 = \int_{-h/2}^{h/2} \sigma_1(\zeta)\zeta\, \mathrm{d}\zeta$, $M_2 = \int_{-h/2}^{h/2} \sigma_2(\zeta)\zeta\, \mathrm{d}\zeta$, $M_{12} = \int_{-h/2}^{h/2} \tau(\zeta)\zeta\, \mathrm{d}\zeta$, in view of (4), we have $M(\alpha) = M_1 \cos^2\alpha + M_2 \sin^2\alpha + M_{12} \sin 2\alpha$.

Now, let us exclude that the normal force may be 0 in all directions at any point in the vault, or in other words, that the equalities $N_1 = N_2 = N_{12} = 0$ hold. For each $\alpha \in [-\pi/2, \pi/2)$, let us define the eccentricity corresponding to direction α,

$$e(\alpha) = \frac{M(\alpha)}{N(\alpha)}. \tag{5}$$

Function $e(\alpha)$ is well defined and continuous whenever $N(\alpha) \neq 0$. Moreover, as has been proved in [20], if there exists $\bar{\alpha}$ such that $N(\bar{\alpha}) = 0$, then $e(\alpha)$ is a constant function. For

each point (η_1, η_2) of the mean surface, let $\alpha_0 \in [-\pi/2, \pi/2)$ be the value of α (not necessarily unique) for which the function $|e(\alpha)| = \left|\frac{M(\alpha)}{N(\alpha)}\right|$ reaches its maximum value. The quantity

$$\tilde{e} = \frac{M(\alpha_0)}{N(\alpha_0)} \tag{6}$$

is the maximum modulus eccentricity at point (η_1, η_2) [20]. The *maximum modulus eccentricity surface* (m.m.e.s.) is thus the set of all points with co-ordinates $(\eta_1, \eta_2, \tilde{e}(\eta_1, \eta_2))$. Wherever two values α_0 and α_1 exist which maximise the function $\left|\frac{M(\alpha)}{N(\alpha)}\right|$ with $\frac{M(\alpha_0)}{N(\alpha_0)} = -\frac{M(\alpha_1)}{N(\alpha_1)}$, the maximum modulus eccentricity surface is not defined.

In the particular case, frequently encountered in the applications, in which the geometry of the vault and the loads have axial symmetry, then the eccentricity can only attain its maximum modulus in the direction of parallels or meridians [20].

It is important to note that, analogous to the line of thrust in the case of arches [21], the m.m.e.s. corresponding to a negative semi-definite stress field is entirely contained within the vault. In fact, we have

$$|M(\alpha)| = \left|\int_{-h/2}^{h/2} \sigma(\alpha,\zeta)\zeta \, \mathrm{d}\zeta\right| \le \int_{-h/2}^{h/2} |\sigma(\alpha,\zeta)\zeta| \, \mathrm{d}\zeta \le \frac{h}{2}\int_{-h/2}^{h/2} |\sigma(\alpha,\zeta)| \, \mathrm{d}\zeta = \frac{h}{2}|N(\alpha)|, \tag{7}$$

where the next to last step is justified by the fact that $\sigma(\alpha,\zeta) \le 0$ for each α and ζ.

Moreover, if the m.m.e.s. is tangent to the extrados or intrados along a path, this path can be considered the site of cylindrical hinges. The corresponding rotational axis coincides with the direction orthogonal to that direction for which the modulus of eccentricity is maximum. Therefore, under the hypotheses usually accepted for arches (namely, that masonry possesses infinite compressive strength and sliding failure cannot occur), as the load increases, vault collapse occurs when the m.m.e.s. is tangent to the intrados and extrados along paths so as to determine a hinge distribution sufficient to render the vault a kinematically indeterminate structure. Thus, in dealing with equilibrium problems, the

m.m.e.s. corresponding to internal forces equilibrated with the load can be used to define a geometrical safety factor similar to that employed for arches [22].

3. Buti's bell tower

3.1 Brief historical account

The centuries-old bell tower of Buti is located in the Pisa mountains. It presents signs of various architectural styles. Stratigraphic analyses of the masonry walls and thorough archive research have highlighted that the structure has changed many times over the course of history. The tower has built during the Middle Ages, in the late XIth century – early XIIth century. This original part of the structures is 26 m high and still standing today. Then during the Renaissance the tower's height was increased to 28 m by addition of a belfry. Further modifications came about during the Baroque period, when an octagonal tambour and vault were added.

Thus, over the centuries the bell tower has undergone considerable changes from a structural point of view. These modifications have had the effect, not only of increasing its weight, but also altering the stress field in some parts of the structure as well.

3.2 Description of the geometry

Buti' bell tower is a square-based prism surmounted by an octagonal brickwork tambour, which supports a vault, for a total height of 34 m. Its external dimensions vary from about 6,9 m x 6,75 m at the base, to 6,5 m x 6,5 m at the belfry level. The stonework of the bell tower is made of *verrucano* stone, a white-rose quartzite, probably mined from local quarries.

Figure 1. Buti's bell tower.

The walls are 1,68 m thick at the base, but taper to 1 m at 22 metre's height, due to two offsets in the masonry within the construction and a gradual reduction in thickness up to the belfry. The northern and eastern sides are free-standing, while the south abuts the church, and a building leans against the west side, up to a height of 11 m.

A brick cross vault was built at a height of about 22 m, and acts as the floor of the belfry. This latter is square in cross section, with about 4,5 m sides and a thickness 1 m. It is made of stone masonry complemented by brickwork. Four gothic style, bricks-lined double lancet windows open on each of the bell tower's sides. An 2 m-high octagonal tambour, with a thickness of about 0,45, m is set on the square-based prism by means of four brick brackets located on the vertices of the prism. The tambour supports the vault, which has diameter of about 5 m, and thickness of a header. The vault is strengthened by ribs and has a lantern set at its top.

3.3 Crack distribution within the structure

Several parts of the bell tower, particularly the masonry structure, are in a clear state of deterioration. Externally, the facing walls of all four sides of the structure bear longitudinal full-width cracks running from the base of the bell tower up to the belfry (Figures 2, 3 and 4). These cracks are also clearly visible from the inside (Fig. 4), and some of them bear the marks of previous stuccoworks testifying to their evolution over time. The stone architraves of the original openings, made of verrucano blocks, presents cracks over one centimetre wide, some of which have been filled with mortar and subsequently reopened.

Figure 2. Crack distribution in the bell tower, external side.

Figure 3. Crack distribution through the clock.

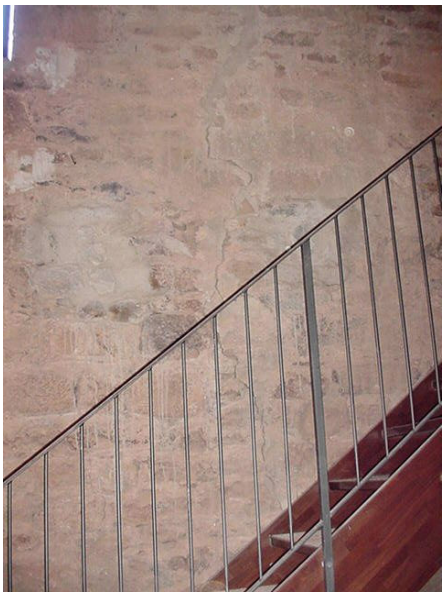

Figure 4. Crack distribution in the bell tower, internal side.

On the southern side (Fig. 3) the vertical crack running along the wall in its centre splits the clock-face above into two parts, and reaches the pentagonal architrave of the original main entrance below. The stuccowork is made from different kinds of mortar, thereby allowing the cracks to be dated to remote times. As for the belfry, wide cracks are visible in the pointed arches, at the crown, as well as in the round arches, at the haunches. Moreover, many bricks have clearly undergone detachment. The vault does not exhibit any clear signs of cracking.

On the whole, the bell tower presents neither significant deformations, nor deviations of the edges from the vertical, nor even yielding or rotations of the structure.

4. Finite-element analysis of the bell tower

Two kinds of finite-element analyses have been performed: in the first case, the bell tower was discretised using eight-nodes brick elements, while in the second, shell elements were employed, with the aim of focusing attention on the behaviour of the vault. For the sake of brevity, henceforth, we shall refer to the analysis conducted using brick elements as analysis 1, and that conducted with shell element as analysis 2.

In analysis 1 the bell tower was discretised with 2920 elements, corresponding to 2135 nodes and 6405 degree of freedom (Figure 5). The geometry of the finite-element model coincides with the geometry of the construction. The thickness of the masonry varies from 1,68 m at the base to 1 m at the level of the belfry, while the belfry has a constant thickness of 1 m. The tambour of the vault was divided into three rings of 0,8 m height and a constant thickness of 0,35 m. The vault was discretised with 192 variable thickness elements, from a maximum of 0,35 m to a minimum of 0,11 m at the top. For the sake of simplicity, the lantern has not been modelled, but accounted for by applying a load equal to the its weight distributed on the top of the vault.

In analysis 2 the bell tower has been discretised with 824 elements.

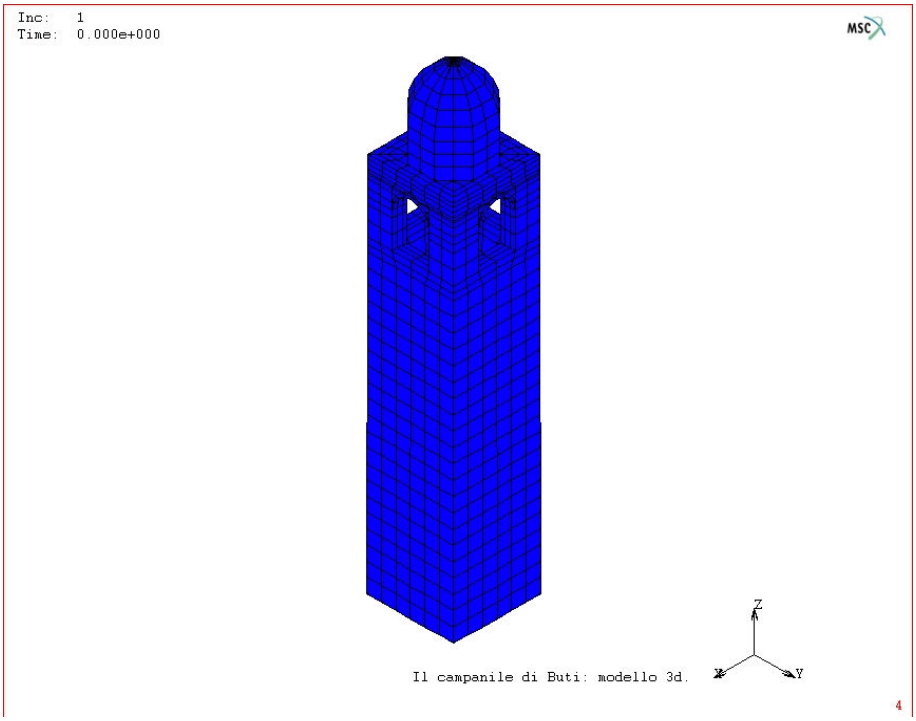

Figure 5. The bell tower, finite-element mesh.

As for the boundary conditions, the base of the bell tower is fixed and the contribution of adjoining constructions assumed to be negligible; consequently, they have not been considered in the analysis.

Two load distributions have been considered. In the first case the bell tower was studied under the action of its own weight; while in the second case, an equivalent static analysis was conducted, in which the bell tower is subjected to its weight as well as a horizontal load that models a seismic action. Such loads were assigned incrementally, the following specific weights have been considered

$p = 1800$ daN/ m^3 for the brick masonry of the tambour and vault,

$p = 2000$ daN/ m^3 for the *verrucano* stone masonry and bricks making up the belfry,

$p = 2200$ daN/ m^3 for the *verrucano* stones of the vertical walls.

The weight of the lantern is 800 daN.

The static load equivalent to an earthquake has been calculated on the basis of the Italian ministerial decree 16-1-1996 [17]. The seismic action is assumed to be a system of horizontal forces acting along the x direction. The vertical effects of the earthquake are neglected. The resultant of the horizontal forces is given by the expression

$$F_h = C \cdot R \cdot I \cdot W,$$

with

$C = \dfrac{S-2}{100}$ the seismic intensity coefficient,

S = 9 the seismicity degree of the site,

R = 1 the response coefficient relative to the direction of the forces,

I = 1 the coefficient of seismic protection,

W = 1673000 daN the weigth of the structure.

Thus, it holds that F_h = 117110 daN.

In analysis 1 the load is uniformly distributed along the x direction on the shaft and belfry; the corresponding force per unit area is $s = \dfrac{117{,}11}{27\text{x}6{,}13} = 0{,}708 \ \dfrac{\text{t}}{\text{m}^2} = 0{,}0708 \ \text{daN/cm}^2$.

At the first increment the weight of the structure has been applied; subsequently, the horizontal load has been split into 100 increments.

In analysis 2, the horizontal load is applied to the whole structure as a force per unit volume, $v = 1{,}5326 \ 10^{-3} \ \text{daN/cm}^3$.

In both analyses, Young's modulus and the Poisson's ratio have been assumed to be same for all the materials making up the bell tower. In particular, we have taken E = 32000 daN/cm^2 and $\nu = 0{,}1$.

Figure 6 shows the x component of the displacement field in the structure subjected to its own weight. The displacement of the shaft is a few mm, and the maximum values are reached at the top of the belfry and at the base of the vault, where they reach about 0,015 mm. Due to the symmetry of both the geometry and loads, the y component of the

displacement behaves in a similar fashion. As for the *z* component, the maximum lowering is experienced by the top of the vault and the keystone of the window arches. The displacement of the top of the vault is about 0.015 m, and that of the arches' keystone exceeds 0,02 m (fig. 7). By inspecting the structure of the windows, it can be observed that the double lancet window is not well toothed to the round arch that bounds the window (Figure 1). This fact suggests that the double lancet windows were added to the round arches some time after the tower's constructions, probably with the aim of containing the strains of the round arches, like a prop.

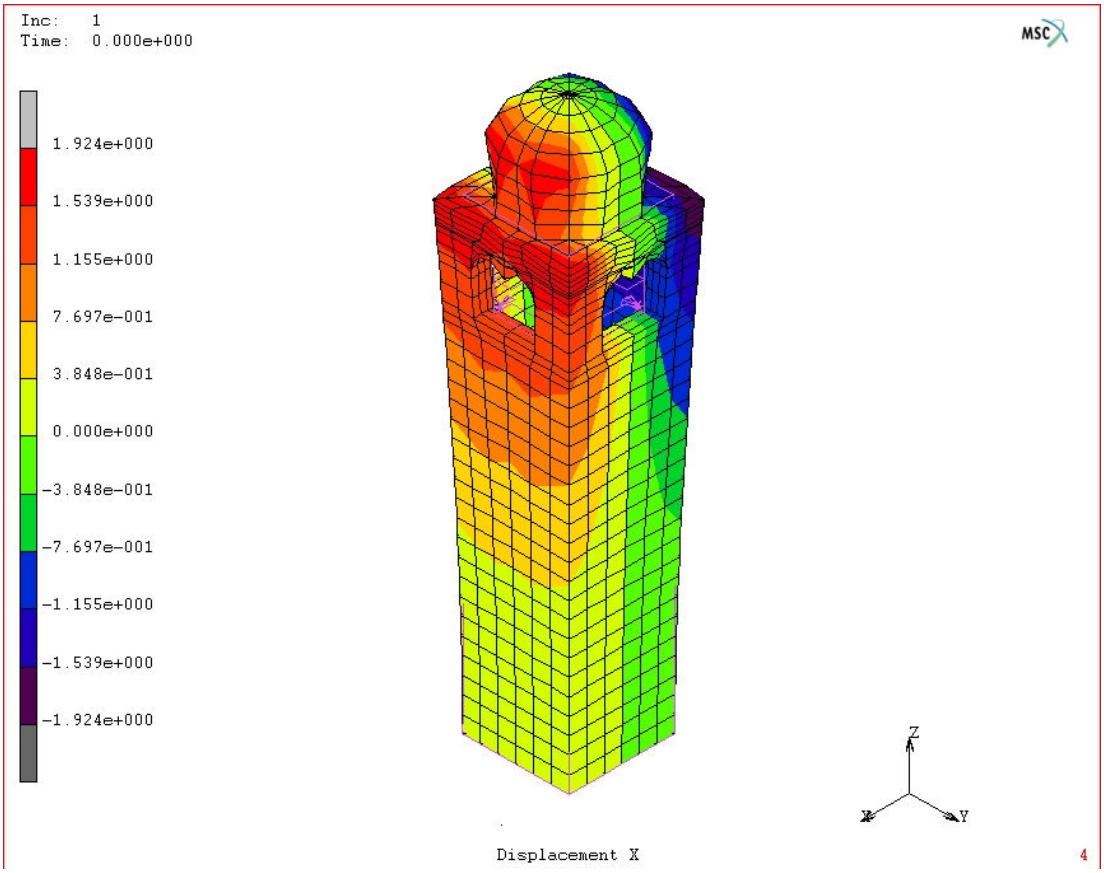

Figure 6. Displacement u_x due to the structure's own weight (load increment 1).

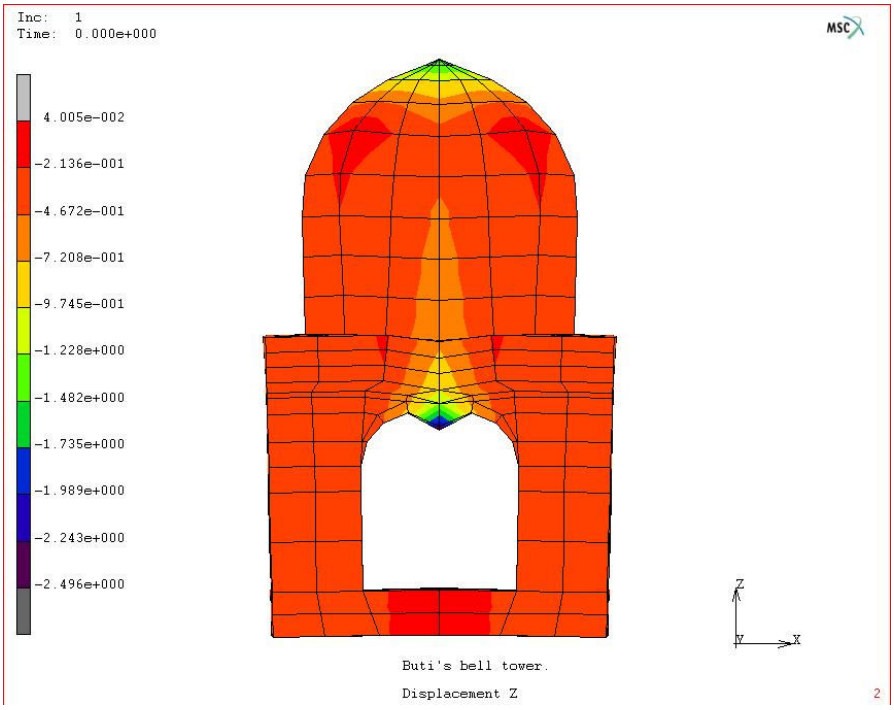

Figure 7. Displacement u_z of the arch (load increment 1).

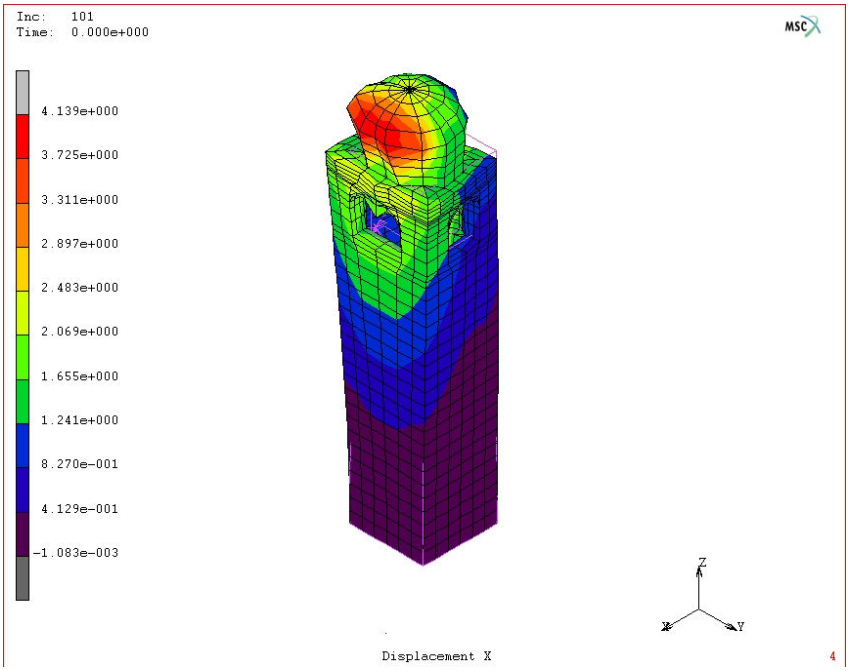

Figure 8. Displacement u_x due to the structure's own weight and the horizontal load (load increment 101).

If the horizontal seismic load is then accounted for, the lowering at the crown increases to about 0,035 m. As for the *x* component of the displacements, the maximum value is reached near the base of the vault, in the same direction of the seismic load and equals 0,037 m (Figure 8).

Let us now analyse the stress field due to the weight. At the first increment, component σ_{zz} of the stress tensor takes on values far lower than the compressive strength of the material. The tower's base, in particular the vertices of the external faces, bear the maximum compressive stresses, whose values are around 9 daN/cm^2 (Figure 9). Stress peaks are limited to the springings of the window arches; where the value of σ_{zz} is 17 daN/cm^2, still below the compressive strength of masonry. In the presence of the horizontal load, the stresses reach values of 17 daN/cm^2 at the leeward vertices of the base, while the windward vertices are subjected to a decrease in stress, down to about 3 daN/cm^2 (Figure 10).

The stress field calculated by NOSA matches the crack distribution in the bell tower quite well; no crushing fractures are presents in any region of the structure, then, the compressive strength is not reached anywhere. The numerical analysis indicates the presence of fractures in the shaft, in particular Figures 11a and 11b show the crack distribution in the leeward wall orthogonal to the seism direction. By using the procedure described at the end of Section 2.1, vertical fractures are revealed in the same positions of the fractures actually existing in the bell tower (Figures 2 and 3), precisely, in the middle of the wall (Figure 11a) and at the haunches of the round arch (figure 11b).

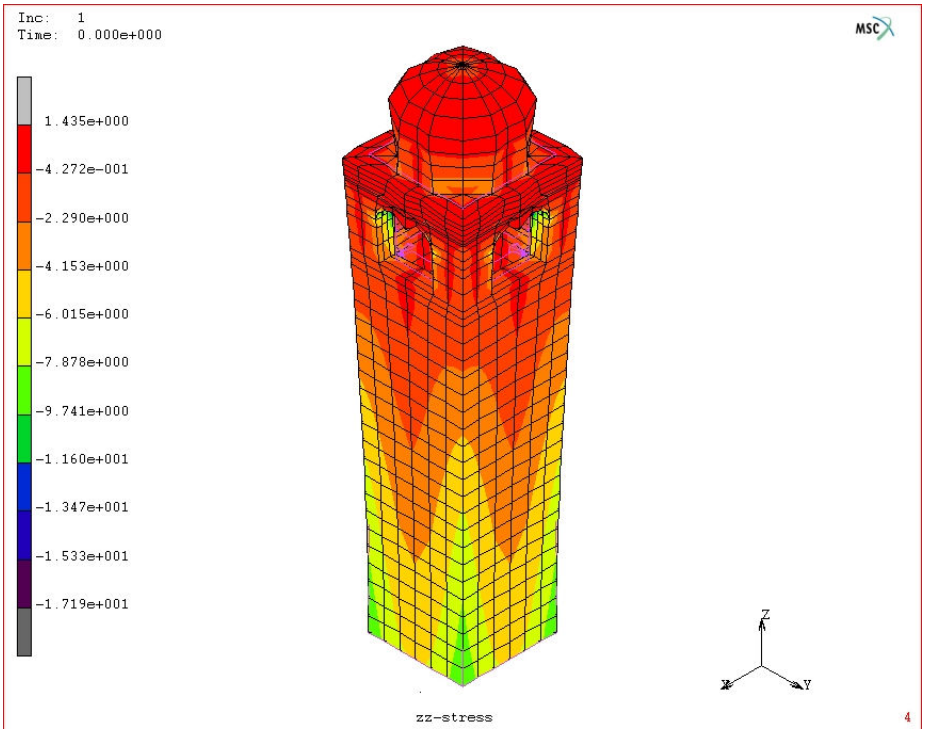

Figure 9. Stress component σ_{zz} at load increment 1.

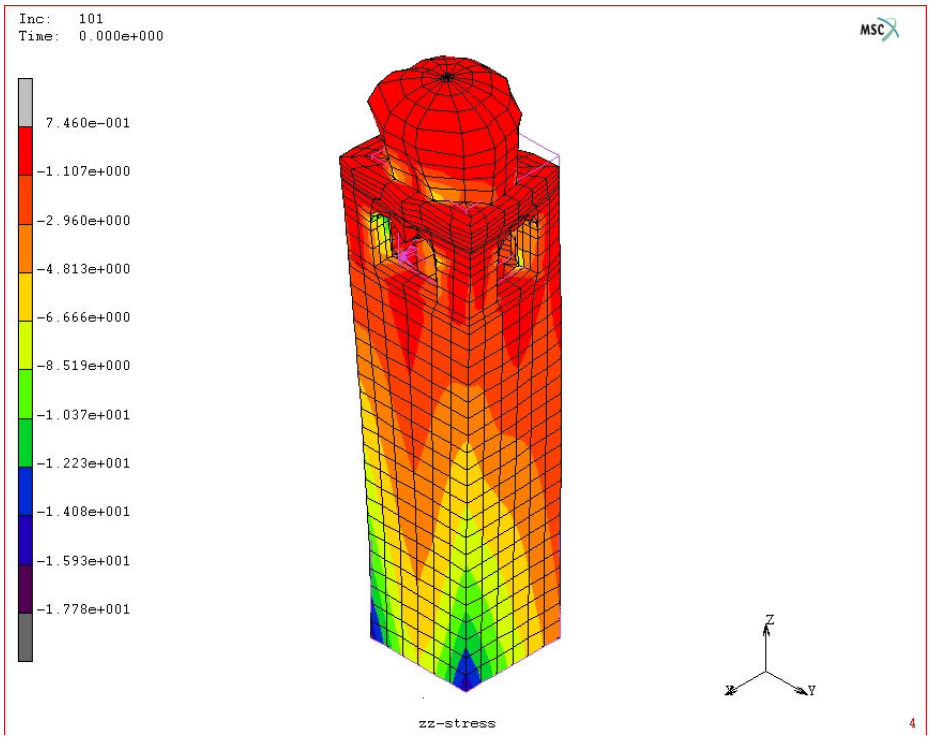

Figure 10. Stress component σ_{zz} at load increment 101.

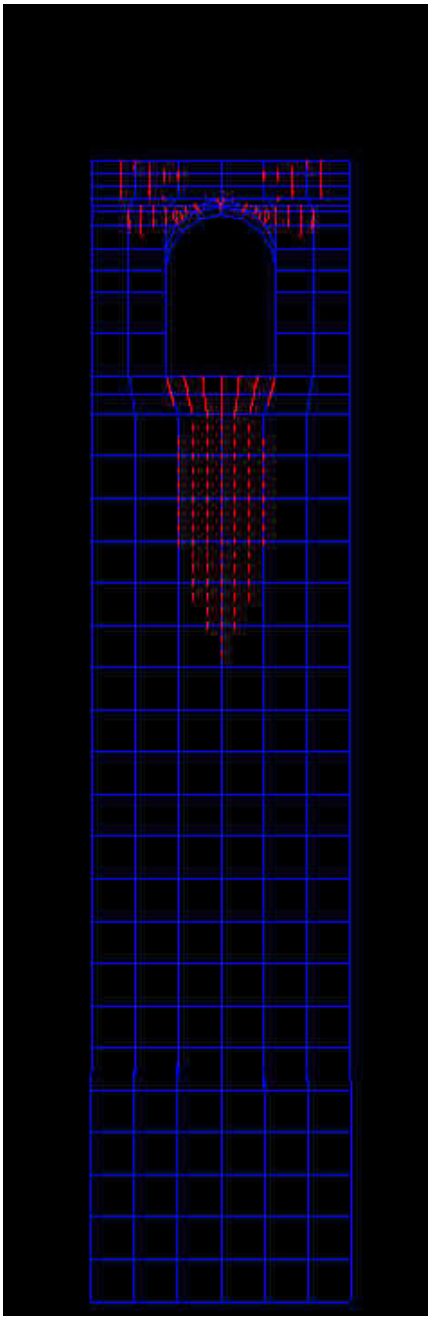

Figure 11a. Cracks in the shaft at load increment 101.

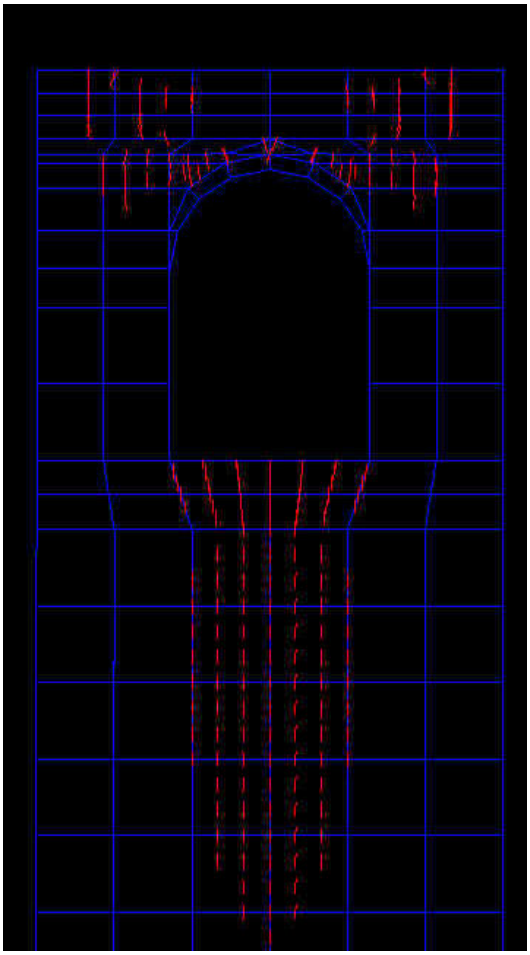

Figure 11b. Particular of Fig. 11a.

The results of analysis 2 are similar to those of analysis 1. However, using shell elements has allowed the behaviour of the vault to be studied as well. The actual bell tower vault has no fractures. The numerical results confirm this situation: Figure 12 depicts the maximum modulus eccentricity surface in a web, when the structure is subjected to its own weight. Figure 13 shows the behaviour of the line of thrust in a section of the vault, obtained via intersection the middle of two opposite webs with a vertical plane. The line of thrust is entirely contained within the middle third of the vault. The results of the numerical analysis conducted by applying the horizontal seismic load reveal that the maximum modulus eccentricity surface continues to be contained within the middle third.

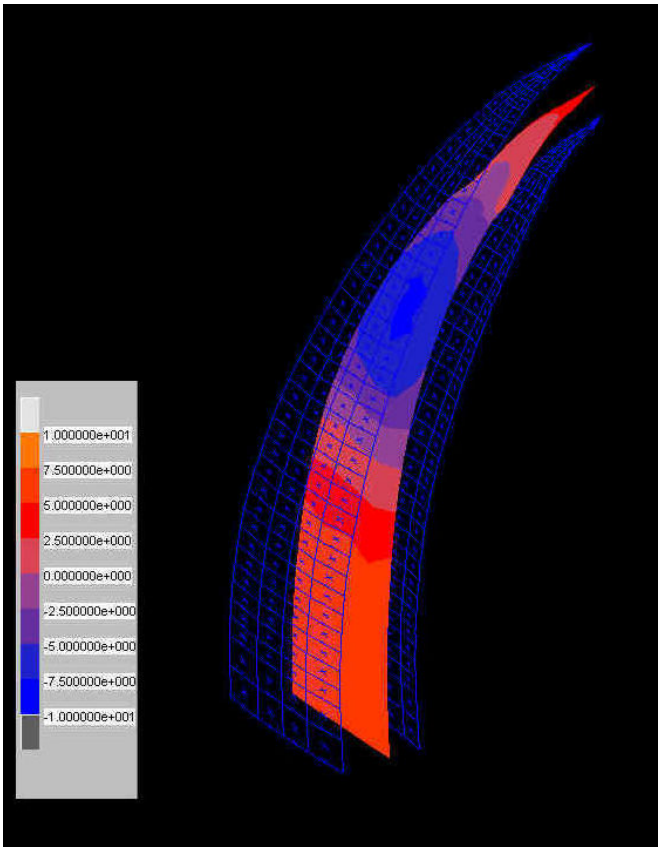

Figure 12. Maximum modulus eccentricity surface in a web of the vault under the action of its own weight.

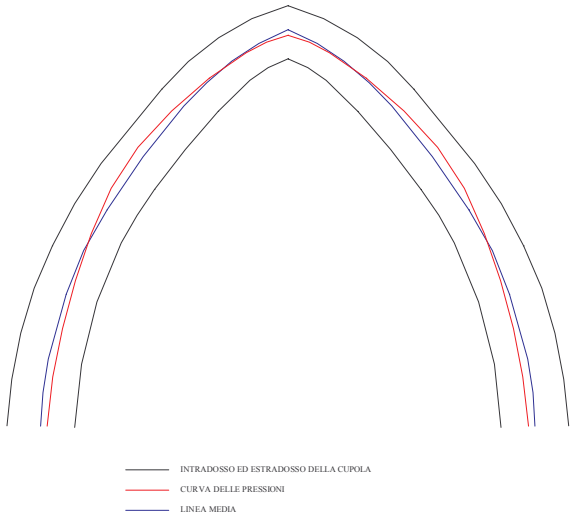

Figure 13. Line of thrust (red line) in a section of the vault under the action of its own weight.

5. Conclusions

After describing the numerical techniques implemented in the finite-element code NOSA for structural analysis of masonry constructions, we exemplify application of the code in an analysis of Buti's bell tower, a deteriorating medieval structure located in the Pisa mountains. Two different analyses have been performed: firstly, with the bell tower subjected to its own weight alone, and then with the structure subjected to both its own weight and a horizontal load, which models a seismic action.

The numerical results obtained via NOSA are in good agreement with the actual distribution of cracking in the bell tower.

Finite-element modelling is an useful tool for understanding the causes of crack formation on masonry structures. In particular, this study has highlighted the importance of numerical analysis in the process of structural recovery and reinforcement of age-old masonry constructions. In fact, as application of the NOSA code allows modelling several possible

strengthening strategies and consequently, determining the response of the structure to each, it can guide the choice of the most suitable consolidation operations for a specific structure.

Acknowledgment. The financial support of the Progetto Finalizzato Beni Culturali of CNR is gratefully acknowledged. The authors would like to express their gratitude to Nicola Zani, who implemented the graphics code used for drawing figures 11a, 11b, 12 and 13.

References

[1] Di Pasquale S., Statica dei solidi murari: teoria e applicazioni, Rapporto Interno Dipartimento di Costruzioni, Università di Firenze, 1984.

[2] Del Piero G., "Constitutive equation and compatibility of the external loads for linearly-elastic masonry-like materials", *Meccanica*, **24** pp. 150-162, 1989.

[3] Sacco E., "Modellazione e calcolo di strutture in materiale non resistente a trazione", *Rend. Mat. Acc. Lincei*, s. 9, v. **1** pp. 235-258, 1990.

[4] Lucchesi M., Padovani C., Pagni A., "A numerical method for solving equilibrium problems of masonry-like solids". *Meccanica* **29**, pp. 175-193, 1994.

[5] Lucchesi M., Padovani C., Pasquinelli G., "On the numerical solution of equilibrium problems of elastic solids with bounded tensile strength". *Comput. Methods Appl. Mech. Engrg.* **127**, pp. 37-56, 1995.

[6] Lucchesi M., Padovani C., Zani N., "Masonry-like solids with bounded compressive strength". *Int. J. Solids Structures* Vol. **33**, No. 14, pp. 1961-1994, 1996.

[7] Alfano G., Rosati L., Valoroso N., "A numerical strategy for finite element analysis of no-tension materials". *Int. J. Numer. Meth. Engng* Vol. **48**, pp. 317-350, 2000.

[8] Degl'Innocenti S., Lucchesi M., Padovani C. , Pagni A., Pasquinelli G., Zani N., "The finite element code NOSA. User's Manual". Technical Report CNUCE ZC 236-94, 1994.

[9] Lucchesi M., Padovani C., Pagni A., Pasquinelli G., Zani N., "COMES-NOSA A finite element code for non-linear structural analysis". Report CNUCE-B4-2000-003.

[10] Pasquinelli G., “On the modeling of the reinforcement rings in masonry buildings: an example”. Proceedings of the Third International Conference on Contact Mechanics, Madrid 1997.

[11] Lucchesi M., Zani N., “Analisi sismica di tipo statico della ciminiera dei Vecchi Macelli, via Nicola Pisano (Pisa)” Relazione Tecnica Consorzio Pisa Ricerche, 29/4/1997.

[12] Lucchesi M., Padovani C., Zani N., “Studio del comportamento statico di alcuni elementi strutturali della Chiesa Madre S. Nicolò di Noto“. Relazione Tecnica Consorzio Pisa Ricerche, 9/3/1998.

[13] Lucchesi M., De Falco A., Zani N., “Studio del comportamento statico dell’arco scenico del teatro Goldoni di Livorno”, Relazione Tecnica Consorzio Pisa Ricerche, 1998.

[14] Lucchesi M., Zani N., “Analisi sismica di tipo statico dell’Arsenale Mediceo situato in Pisa, lungarno Simonelli”, Relazione Tecnica Consorzio Pisa Ricerche, 1996.

[15] Cecati F., Lucchesi M., Padovani C., Pagni A., Zani N., “Consolidamento e adeguamento antisismico: un modello di calcolo per orientare il progetto”. *XIV Convegno Scienza e Beni Culturali*, Bressanone, 30 giugno-3 luglio, 1998.

[16] Lucchesi M., Padovani C., Pasquinelli G., Zani N., “Static analysis of masonry vaults”, submitted to ASCE JEM, 2002.

[17] D.M. 16 gennaio 1996 “Norme tecniche per le costruzioni in zone sismiche”.

[18] Guidotti P., Lucchesi M., Pagni A., Pasquinelli G., Application of Shell Theory to Structural Problem Using the Finite Element Method, Quaderni de "La Ricerca Scientifica" del CNR, 115, 1986.

[19] Padovani C., Pasquinelli G., Pagni A. “Gli elementi guscio nel codice agli elementi finiti NOSA”. Rapporto CNUCE-B4-1998-012, luglio 1998.

[20] Lucchesi M., Padovani C., Pasquinelli G., Zani N., “The maximum modulus eccentricity surface for masonry vaults and limit analysis”. *Mathematics and Mechanics of Solids* **4**, pp. 71-87, 1999.

[21] Lucchesi M., Padovani C., Pasquinelli G., Zani N., “On the collapse of masonry arches”. *Meccanica* **32**, pp. 327-346, 1997.

[22] Heyman J., The Masonry Arch. J. Wiley & Sons, 1982.